nature portfolio

Peer Review File

Quantum geometry quadrupole-induced third-order nonlinear transport in antiferromagnetic topological insulator MnBi2Te4

Reviewers' Comments:

Reviewer #1:

Remarks to the Author:

The manuscript by Li et a!. presents third-order nonlinear response observed in topological antiferromagnet MnBi2Te4 both at longitudinal and transverse directions. The nonlinear response (V_xx^3ω and V_xy^3ω) exhibit abrupt changes corresponding to the transition of the magnetic state in MnBi2Te4. Notably, the measured V_xx^3ω is identified as an even function of the magnetic field B, while V_xy^3ω displays an odd function of B. The authors claim that V_xx^3ω is induced by the quantum metric quadrupole, and V_xy^3ω originates from the Berry curvature quadrupole. Recently, the investigation of nonlinear transport responses has gained significant attention due to their connection to quantum geometry.

Even though I believe their results are intriguing, the following issues need to be resolved in order to improve the manuscript.

1. The third-order nonlinearity can also be induced by Berry connection polarizability tensor in centrosymmetric materials, which has been observed in MoTe2 (S. Lai, et a!. Nature Nanotechnology 16, 869–873 (2021)). Could the authors exclude the effect from Berry connection polarizability tensor?

2. The authors cited the theory paper (C. P. Zhang, et a!. PRB 107, 115142 (2023)) to support their conclusion that the observed nonlinear response originates from quantum metric and Berry curvature quadrupole. This theoretical study also indicates that the high-order nonlinear response can arise from the Drude-like tensor and impurities. Have the authors considered excluding the effects of these factors in their analysis?

3. The scaling law is considered an effective method for exploring the microscopic origin and mechanism of linear or nonlinear anomalous Hall effects. Given that quantum metric is believed to contribute at Tau^0 to nonlinear transport responses (A. Gao, et a!. Science 381, 181-186 (2023), and N. Wang, et a!. Nature 621, 487-492(2023)) and Berry curvature dipole depends on Tau^1 (K. Kang, et a!. Nature materials 18, 324-328(2019)), could the authors investigate the scaling law of the observed third-order nonlinear responses depends with respect to Tau or the longitudinal conductivity Sigma?

4. According to the previous publications on nonlinear transport, it is well-established that the nonlinear response is significantly influenced by the crystal symmetry of materials. Furthermore, the theory paper referenced by the authors indicates the dependence of nonlinear response on crystal symmetry. Could the authors provide results demonstrating the symmetry dependence of the observed third-

order nonlinear response, particularly by measuring the nonlinear response when applying an alternating current along different direction of the $MnBi_2Te_4$?

5. Could the authors present the two-terminal I-V curves of the devices? Is it linear? Additionally, it would be valuable to include data measured between other pairs of contacts on the Hall bar device— do these measurements exhibit consistency?

6. Could the authors show the data measured under different frequencies of alternating current? Is the measured nonlinear response independent of the frequency of driving current.

7. As shown in Figure 3b, the calculated sigma_xxxx contributed by quantum metric does not exhibit a distinct peak when the magnetic state transitions from antiferromagnetic to ferromagnetic. Why there are so sharp peaks observed in V_xx^3ω around ±2.5T at T=2K and 10K curves, as shown in Figure 3a?

8. It seems that there are some periodic oscillations in the V_xy^3ω curves measured at T≥15K in Figure 4a, but no oscillation in the calculated Q_xxz at Figure 4b. Can the authors explain where are these oscillations come from?

9. Given the authors have theoretically calculated magnetic order parameter Δ dependence nonlinear conductivity originating from quantum metric and Berry curvature quadrupole, the authors should compare the experimental nonlinear conductivity with the theoretically calculated results to see if the experimental data are consistent with the theoretical results.

Reviewer #2:
Remarks to the Author:
The manuscript by Li et al presents third-harmonic longitudinal and transverse transport measurements of bulk $MnBi_2Te_4$ as a function of magnetic field and temperature, which suggest transitions between antiferromagnetic (AFM), canted antiferromagnetic (CAF) and ferromagnetic (FM) states. Theoretical calculations suggest that these third order signals arise from quantum geometric quadrupoles.
The observation of third harmonic signals are quite interesting, and the data presented are nice. The quantum geometric quadrupole effect is novel and exciting. Overall I recommend publication by Nature Communications, if the authors address the following:
1. The data presented are very symmetric with respect to B. Are they symmetrized or antisymmetrized? If so, such procedures should be clearly stated in Methods, and raw data shown in Supplement.

2. The color scales in Fig. 1a and 1b should be labelled.
3. The current applied (0.6 mA) is very large, which may be problematic.
a. For typical Rxx~70 ohms, this translates to 40 mV, which is much larger than thermal energy. Thus the electrons may not be in the ground state.
b. How is heating effect excluded? The authors cite ref. 41, which is a PhD thesis. I suggest the authors include in the Supplement a summary of the relevant sections of the thesis and any representative figures.
c. The Supplement shows that the third harmonic signals are non-linear in current. If a smaller current (e.g. 0.1 mA) is used, does T_N or "switching" field change?

Reply to Reviewer #1 (Remarks to the Author):

[General Remark]: "The manuscript by Li *et al.* presents third-order nonlinear response observed in topological antiferromagnet $MnBi_2Te_4$ both at longitudinal and transverse directions. The nonlinear response ($V_{xx}^{3\omega}$ and $V_{xy}^{3\omega}$) exhibit abrupt changes corresponding to the transition of the magnetic state in $MnBi_2Te_4$. Notably, the measured $V_{xx}^{3\omega}$ is identified as an even function of the magnetic field B, while $V_{xy}^{3\omega}$ displays an odd function of $\boldsymbol{B}$. The authors claim that $V_{xx}^{3\omega}$ is induced by the quantum metric quadrupole, and $V_{xy}^{3\omega}$ originates from the Berry curvature quadrupole. Recently, the investigation of nonlinear transport responses has gained significant attention due to their connection to quantum geometry. Even though I believe their results are intriguing, the following issues need to be resolved in order to improve the manuscript."

[Reply]: We thank the reviewer for your overall positive evaluation on our work. As shown in the point-to-point responses below, we have addressed all the comments and suggestions raised by the reviewer with refined discussions and newly-obtained experimental data, and have revised the manuscript accordingly. We appreciate the reviewer's comments, which have substantially improved our work with enhanced validity.

[Remark 1]: "The third-order nonlinearity can also be induced by Berry connection polarizability tensor in centrosymmetric materials, which has been observed in $MoTe_2$ (S. Lai, *et al*. Nature Nanotechnology 16, 869–873 (2021)). Could the authors exclude the effect from Berry connection polarizability tensor?"

[Reply]: We thank the reviewer for this important question. The quantum metric quadrupole and the Berry connection polarizability tensor are closely related. The Berry connection polarizability tensor $G_{ab} = 2Re \sum_{m \neq n} \frac{(\mathcal{A}_a)_{nm}(\mathcal{A}_b)_{mn}}{\varepsilon_n - \varepsilon_m}$ differs from the quantum metric tensor $g_{ab} = Re \sum_{m \neq n} (\mathcal{A}_a)_{nm}(\mathcal{A}_b)_{mn}$ only by a factor of 2 divided by the band gap. Here, ε_n is the energy spectrum, $\mathcal{A}_a$ is the Berry connection, and *a*, *b* are the spatial indices. It is only recently that people have realized the existence of the Berry connection polarizability tensor is indeed closely connected to the quantum metric tensor.

Specifically, under an applied electric field, the nontrivial quantum geometry can induce the ***second order nonlinear conductance*** with the following explicit forms:

$$\sigma_{abc}^{2\omega} = \frac{e^3}{\hbar} \int_{\boldsymbol{k}} \left[-2\partial_a G_{bc} + \frac{1}{2}(\partial_b G_{ac} + \partial_c G_{ab}) \right] f_0 \qquad \text{(Eq. R1)}$$

where $\partial_a \equiv \frac{\partial}{\partial k_a}$ is the derivative with respect to the wave vector. In other words, the first-order derivatives of the Berry connection polarizability tensor G_{ab} can induce the second-order longitudinal nonlinear conductivity and the second-order nonlinear Hall conductivity, as recently been observed in $MnBi_2Te_4$ by A. Gao, *et al* [*Science* **381**, 181–186 (2023)] and N. Wang, *et al* [*Nature* **621,** 487–492 (2023)]. As they correctly pointed out, this is due to the existence of the quantum metric dipole $\partial_a g_{bc}$ of the Bloch electrons in $MnBi_2Te_4$. Indeed, one can rewrite the second order nonlinear conductance in Eq.R1 in terms of the quantum metric dipole $\partial_a g_{bc}$ as done by A. Gao, *et al* [*Science* **381**, 181–186 (2023)].

On the other hand, in terms of the Berry connection polarizability tensor G_{ab}, ***the third order nonlinear conductance*** can be expressed as

$$\sigma_{abcd}^{3\omega} = \frac{e^4\tau}{\hbar^2} \left[\int_{\boldsymbol{k}} (-\partial_a \partial_b G_{cd} + \partial_a \partial_d G_{bc} - \partial_b \partial_d G_{ac}) f_0 + \frac{1}{2} \int_{\boldsymbol{k}} v_a v_b G_{cd} f_0'' \right] \text{(Eq. R2)}$$

where τ is the scattering time and v_a is the group velocity. In our experiment, we have observed the ***third-order nonlinear conductivity*** induced by the second-order derivatives of the Berry connection polarizability tensor as shown in Eq. R2. Similar to the work of A. Gao, *et al* [*Science* **381**, 181–186 (2023)], $\partial_a \partial_b G_{cd}$ can also be written in terms of $\partial_a \partial_b g_{cd}$, which is the quantum metric quadrupole of the Bloch electrons. Therefore, the third-order nonlinear longitudinal conductance observed is induced by the quantum metric quadrupole. Therefore, the third order effect which we observed can be understood from the Berry connection polarizability or from the quantum metric quadrupole. They are the same effects.

[Remark 2]: "The authors cited the theory paper (C. P. Zhang, et al. PRB 107, 115142 (2023)) to support their conclusion that the observed nonlinear response originates from the quantum metric and Berry curvature quadrupole. This theoretical study also indicates that the high-order nonlinear response can arise from the Drude-like tensor and impurities. Have the authors considered excluding the effects of these factors in their analysis?"

[Reply]: We agree with the reviewer that the Drude-like tensor can also contribute to the third-order longitudinal nonlinear conductivity. The C_3 symmetry of $MnBi_2Te_4$ crystal requires the third-harmonic nonlinear ***longitudinal*** conductivity can only come from the quantum metric quadrupole and Drude contributions, while the third-order ***Hall*** conductivity is only contributed by Berry curvature quadrupole (BCQ) and skew scattering. The quantum metric quadrupole and the Drude contribution have different dependence on the scattering time τ. Therefore, we can distinguish them with the scaling law analysis, as the reviewer suggested in the next question.

The third-order nonlinear conductivity $\frac{e^4\tau}{\hbar^2} G_{xxxx}$, which is related to the third order current by $j^{3\omega}_{x,QMQ} = \frac{e^4\tau}{\hbar^2} G_{xxxx} E_x^3$, is related to the quantum metric quadrupole. Here, $G_{xxxx} = -\int_{\boldsymbol{k}} \partial_x^2 G_{xx} f_0 + \frac{1}{2}\int_{\boldsymbol{k}} v_x^2 G_{xx} f_0''$ can be expressed as the integral of the quantum metric quadrupole $\partial_x^2 G_{xx}$ and the (normalized) quantum metric G_{xx}. Recall the linear conductivity from the Drude formula $\sigma_{xx} = \frac{ne^2\tau}{m_{eff}}$, we get the relation between the third-harmonic longitudinal voltage $V_{x,QCQ}^{3\omega}$ and the driving ac voltage $(V_x^{\omega})^3$ as

$$\frac{V_{x,QCQ}^{3\omega}}{(V_x^{\omega})^3} = \frac{1}{L^2}\frac{e^2 m_{eff}}{\hbar^2 n} G_{xxxx} \qquad \text{(Eq. R3)}$$

Here, L, e, $m_{eff,}$ $\hbar$, and n are the length between the voltage probes, elemental charge, effective mass, reduced Plank constant, and carrier density, respectively. Eq. R3 clearly shows that the quantum metric quadrupole induced third-harmonic nonlinear longitudinal voltage is ***independent of the scattering time*** $\boldsymbol{\tau}$ or the longitudinal conductivity σ_{xx}.

On the other hand, the Drude contribution to the third-order longitudinal current is $j_{x,D}^{3\omega} = \frac{e^4\tau^3}{\hbar^4} D_{xxxx} E_x^3$ with $D_{xxxx} = \int_{\boldsymbol{k}} \partial_x^4 \varepsilon(k) f_0$, which yields the third-harmonic nonlinear longitudinal voltage

$$\frac{V_{x,D}^{3\omega}}{(V_x^{\omega})^3} = \frac{1}{L^2}\frac{m_{eff}^3 D_{xxxx}}{e^2\hbar^4 n^3}\sigma_{xx}^2 \qquad \text{(Eq. R4)}$$

Together, we obtain the total third-harmonic nonlinear longitudinal voltage as

$$\frac{V_x^{3\omega}}{(V_x^{\omega})^3} = \frac{1}{L^2}\frac{m_{eff}^3 D_{xxxx}}{e^2\hbar^4 n^3}\sigma_{xx}^2 + \frac{1}{L^2}\frac{e^2 m_{eff}}{\hbar^2 n} G_{xxxx} = \alpha\sigma_{xx}^2 + \beta \qquad \text{(Eq. R5)}$$

Therefore, the slope α is directly related to the Drude-like contribution, while the intercept β characterizes the quantum metric quadrupole contribution.

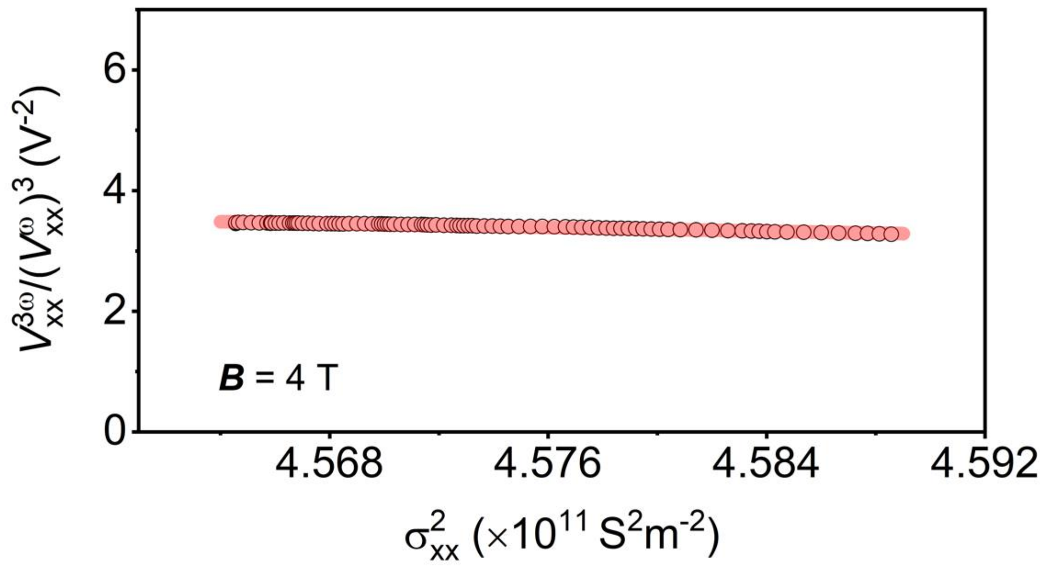

Fig. R1 The nonlinear longitudinal voltage $\frac{V_x^{3\omega}}{(V_x^{\omega})^3}$ as a function of square of the linear conductivity σ_{xx}^2 at ***B*** = 4 T and *T* < 10 K for bulk $MnBi_2Te_4$. The red line is the linear fitting curve.

The fitting of Eq. R5 to the experimental data shown in Fig. R1 yields $\alpha = (-7.91 \times 10^{-11} \pm 1.01 \times 10^{-12})\, V^{-2}\Omega^2\mathrm{m}^2$ and $\beta = (39.58 \pm 0.46)\, V^{-2}$. At low temperatures with $\sigma_{xx} = 6.76 \times 10^5\ S/m$, we find the Drude-like contribution $\alpha\sigma_{xx}^2 = -36.11\, V^{-2}$ is comparable with the quantum metric quadrupole contribution $\beta = 39.58\, V^{-2}$.

We have added such discussion in Supplementary Note 10 in the revised Supplementary Information and cited in the main text on page 10, which reads "*Furthermore, the scaling law analysis suggests the third-harmonic longitudinal voltage could be attributed by Drude-like tensor contribution and quantum metric quadrupole with comparable magnitude at low temperatures, as detailed in Supplementary Note 9. However, the Drude-like tensor contribution is insensitive to the magnetic phase transition induced by the external **B**-fields, which indicates the experimental observed **B**-fields dependence of the third-harmonic nonlinear longitudinal voltage in bulk $MnBi_2Te_4$ is mainly contributed by quantum metric quadrupole with a constant background contributed by Drude-like tensor.*"

We thank the reviewer again for this important question.

[Remark 3]: "The scaling law is considered an effective method for exploring the microscopic origin and mechanism of linear or nonlinear anomalous Hall effects. Given that quantum metric is believed to contribute at τ^0 to nonlinear transport responses (A. Gao, et al. Science 381, 181-186 (2023), and N. Wang, et al. Nature 621, 487-492(2023)) and Berry curvature dipole depends on τ^1 (K. Kang, et al. Nature materials 18, 324-328(2019)), could the authors investigate the scaling law of the observed third-order nonlinear responses depends with respect to τ or the longitudinal conductivity Sigma?"

[Reply]: We thank the reviewer's suggestion on the study of the scaling law, which is indeed very important. As mentioned in Reply 2, using the scaling law, we distinguished the quantum metric contribution from the Drude contribution for ***the longitudinal response***. The third order voltage $V^{3\omega}_{x,QCQ}$ originated from the quantum metric quadrupole is indeed independent of τ.

For the ***Hall response*** (the voltage perpendicular to the driving current), the third-order Hall conductivity can only be contributed by the Berry curvature quadrupole (BCQ) and skew scatterings due to the C_3 symmetry of $MnBi_2Te_4$ crystal. The Hall response is not related to the quantum metric terms. Here, we provide the scaling law analysis to distinguish Berry curvature quadrupole contribution from skew scattering, as suggested by the reviewer.

The third-order nonlinear anomalous Hall effect contributed by the Berry curvature quadrupole Q_{xxz} is $j^{3\omega}_{y,BCQ} = \frac{e^4\tau^2}{\hbar^3} Q_{xxz} E^3_x$. Recall that the linear conductivity from the Drude formula $\sigma_{xx} = \frac{ne^2\tau}{m_{eff}}$, we get the third-harmonic Hall voltage

$$\frac{V_{y,BCQ}^{3\omega}}{(V_x^{\omega})^3} = \frac{W}{L^3}\frac{m_{eff}^2}{\hbar^3 n^2}Q_{xxz}\sigma_{xx} \quad \text{(Eq. R6)}$$

where W, L, e, m_{eff}, $\hbar$, and n are the width of the device, the length between the voltage probes, elemental charge, effective mass, reduced Plank constant, and carrier density, respectively.

On the other hand, the skew scattering induced third-order nonlinear anomalous Hall current is

$$j_{y,sk}^{3\omega} = -e\int dk\, v_y(k) f_A^{(3)}(k) \quad \text{(Eq. R7)}$$

where $v_y(k) = \frac{1}{\hbar}\partial_y \varepsilon(k)$ is the group velocity, and $f_A^{(3)}(k)$ is the third-order correction to the Fermi-Dirac distribution function by skew scattering. $f_A^{(3)}(k)$ can be estimated as $f_A^{(3)}(k) \sim \frac{\tau}{\bar{\tau}}\frac{e^3\tau^3}{\hbar^3}\partial_x^3 f_0 E_x^3$ [H. Isobe, *et al., Sci. Adv.* **6**, eaay2497(2020)], where $\bar{\tau}$ is the skew scattering time, which yields the nonlinear Hall voltage

$$\frac{V_{y,sk}^{3\omega}}{(V_x^{\omega})^3} \sim \frac{W}{L^3}\frac{m_{eff}^2}{2e^4 n^3 \varepsilon_F \bar{\tau}}\sigma_{xx}^3 \quad \text{(Eq. R8)}$$

Together, we obtain the total third-harmonic nonlinear Hall voltage

$$\frac{V_y^{3\omega}}{\sigma_{xx}(V_x^{\omega})^3} = \frac{W}{L^3}\frac{m_{eff}^2}{2e^4 n^3 \varepsilon_F \bar{\tau}}\sigma_{xx}^2 + \frac{W}{L^3}\frac{m_{eff}^2}{\hbar^3 n^2}Q_{xxz} = \eta\sigma_{xx}^2 + \xi \quad \text{(Eq. R9)}$$

where we have divided the nonlinear Hall voltage with a factor of σ_{xx} for the benefit of the fitting.

The fitting of Eq. R9 to the experimental data is shown in Fig. R2 and yields $\eta = (5.79 \times 10^{-17} \pm 9.32 \times 10^{-19})\ V^{-2}\Omega^3\mathrm{m}^3$ and $\xi = (-2.73 \times 10^{-5} \pm 4.26 \times$

10^{-7}) $\mathrm{V}^{-2}\Omega$m. Considering $\sigma_{xx} = 6.76 \times 10^5\ S/m$ at low temperatures, we find the skew scattering contribution $\eta\sigma_{xx}^3 = 17.88\ V^{-2}$ is comparable in magnitude with the Berry curvature quadrupole contribution $\xi\sigma_{xx} = -18.45\ V^{-2}$.

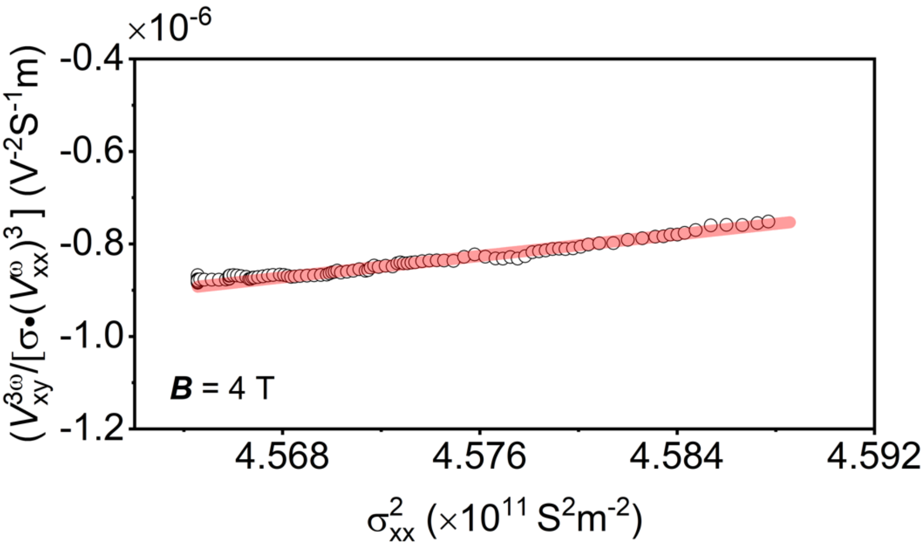

Fig. R2 The nonlinear transverse voltage $\frac{V_{xy}^{3\omega}}{\sigma_{xx}(V_x^{\omega})^3}$ as a function of square of the linear conductivity σ_{xx}^2 at ***B*** = 4 T and *T* < 10 K for bulk $MnBi_2Te_4$. The red line is the linear fitting curve.

We have added such discussion in the Supplementary Note 9 in the revised Supplementary Information and cited in main text on page 11, which reads "*It is noted that the skew scattering may also contribute to the third-harmonic transverse voltages. As detailed in the scaling law analysis in Supplementary Note 9, the magnitude of skew scattering contribution is calculated to be comparable to that of the Berry curvature quadrupoles. However, the skew scattering contribution should be insensitive to the external B-fields, the dependence on the order parameter Δ strongly reinforces our claim of observing the third-harmonic transverse nonlinear conductivity stemming from the Berry curvature quadrupoles contributions.*"

[Remark 4]: "According to the previous publications on nonlinear transport, it is well-established that the nonlinear response is significantly influenced by the crystal symmetry of materials. Furthermore, the theory paper referenced by the authors indicates the dependence of nonlinear response on crystal symmetry. Could the authors provide results demonstrating the symmetry dependence of the observed third-order nonlinear response, particularly by measuring the nonlinear response when applying an alternating current along different direction of the $MnBi_2Te_4$?"

[Reply-V1]: We thank the reviewer for this insightful question. The symmetry properties of the quantum metric quadrupole and Berry curvature quadrupole are indeed very different from the symmetry properties of the second order nonlinear Hall effect **[**I. Sodemann and L. Fu, Phys. Rev. Lett. **115**, 216806 (2015)]. The second order nonlinear Hall effect induced by Berry curvature dipole can exist ***only*** if the crystal symmetry is so low that only a single (vertical) mirror plane is allowed. Moreover, the second order Hall voltage is proportional to dot product of the Berry curvature dipole and the applied electric field [I. Sodemann and L. Fu, Phys. Rev. Lett. **115**, 216806 (2015)]. Therefore, the second order Hall voltage vanishes when the current direction is perpendicular to the Berry curvature dipole direction as observed in the experiment in T_d-WTe_2 [K. Kang *et al.*, *Nature Materials* **18**, 324-328(2019)].

However, for the third order nonlinear Hall effect induced by quantum metric quadruple and Berry curvature quadrupole, the symmetry property is richer. As shown in our previous theoretical work, the higher order nonlinear Hall effect can appear in 66 magnetic point groups [C. P. Zhang, *et al.*, *Phys. Rev. B* 107, 115142 (2023)]. For $MnBi_2Te_4$, due to the preservation of inversion symmetry of the bulk, the second order nonlinear Hall effect is zero which is consistent with our measurements. For the third order nonlinear Hall effect induced by Berry curvature quadrupole, the effect is finite even with inversion symmetry. Interestingly, due to the C_3 symmetry of the crystal, both the third order longitudinal and Hall voltages are expected to be isotropic in all current directions.

In the experiment, we are not able to make a perfectly circular device. In this case, the effect of the geometric shape of the device can not be ignored as the measured voltage depends on the effective length and width of the sample, which change as the current direction changes.

We have measured the angular-resolved nonlinear response of the bulk $MnBi_2Te_4$, as shown in Fig. R3 below. Fig. R3a shows the optical image of the device, where the bulk $MnBi_2Te_4$ was transferred on the circular twelve electrodes and was capped with a thin h-BN film. The angular dependent first- and third-harmonic current-voltage characteristics are measured. The definition of the angle θ is indicated by the yellow arrows where the short yellow arrow denotes $\theta = 0$. The first-harmonic resistance is almost a constant of ~55 Ω, as shown in Fig. R3b. The slight variation with the angle is due to the geometric shape effect as the $R_{xx}^{\omega} \propto \frac{L}{W}$ where L and W are the effective length and width of the sample, respectively.

The solid orange circles in Fig. R3c and solid blue squares in Fig. R3d show the calculated scaling factor $V_{xx}^{3\omega}/(V_{xx}^{\omega})^3$ and $V_{xy}^{3\omega}/(V_{xx}^{\omega})^3$ as a function of the angles, respectively. As can be seen, the third-harmonic longitudinal and transverse scaling factors are nearly constant with slight angle dependence. This slight variations with the angles can be caused by the fact that the longitudinal scaling factor $\frac{V_{xx}^{3\omega}}{(V_{xx}^{\omega})^3} \propto \frac{1}{L^2}$ and the transverse scaling factor $\frac{V_{xy}^{3\omega}}{(V_{xx}^{\omega})^3} \propto \frac{W}{L^3}$. As shown in Fig.R3c and Fig.R3d, the third order nonlinear voltages ***do not vanish in all current directions***, which is consistent with the C_3 symmetry of the crystal.

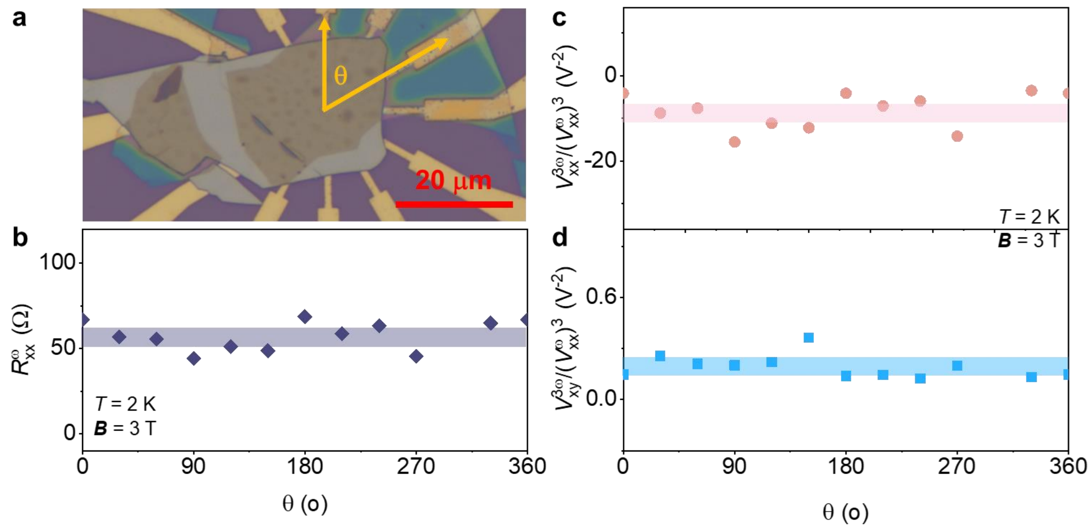

Fig. R3. Angular-resolved third-harmonic nonlinear transport properties of bulk $MnBi_2Te_4$. (a) Optical image of the bulk $MnBi_2Te_4$. The bulk $MnBi_2Te_4$ was transferred on the circular electrodes and covered by a thin layer of *h*-BN. The angle θ is indicated by the yellow arrows. (b) Angular dependent first-harmonic resistance (solid navy-blue diamond) of the bulk $MnBi_2Te_4$. (c) $V_{xx}^{3\omega}/(V_{xx}^{\omega})^3$ (solid orange circles) and (d) $V_{xy}^{3\omega}/(V_{xx}^{\omega})^3$ (solid blue squares) as a function of the angle between the electrodes. The solid lines are guides for the eyes.

[Remark 5]: "Could the authors present the two-terminal *I*-*V* curves of the devices? Is it linear? Additionally, it would be valuable to include data measured between other pairs of contacts on the Hall bar device-do these measurements exhibit consistency?"

[Reply]: As suggested by the reviewer, we have measured the two-terminal *I*-*V* curves of the devices, as shown in Fig. R4b. As can be seen, all the *I*-*V* curves measured between the two probes of bulk $MnBi_2Te_4$ marked in Fig. R4a are of linear characteristic, which suggests the devices are of good ohmic contact.

We further measured the third-harmonic nonlinear Hall voltage for two pairs of Hall bar, as shown in Fig. R4c. The cyan curve is collected between the Hall bar probes 5-6 and is compared to the previous measurement presented in the main text (purple curve).

The orange curve is measured between the Hall bar probes 3-4. As can be seen, the overall features of the sharp transitions along with the magnetization transition of the bulk $MnBi_2Te_4$ are well reproducible. These results demonstrate a good consistency and reproducibility of the nonlinear transport measurements in our work. We have added these measurements in the revised Supplementary Information as Fig. S2.

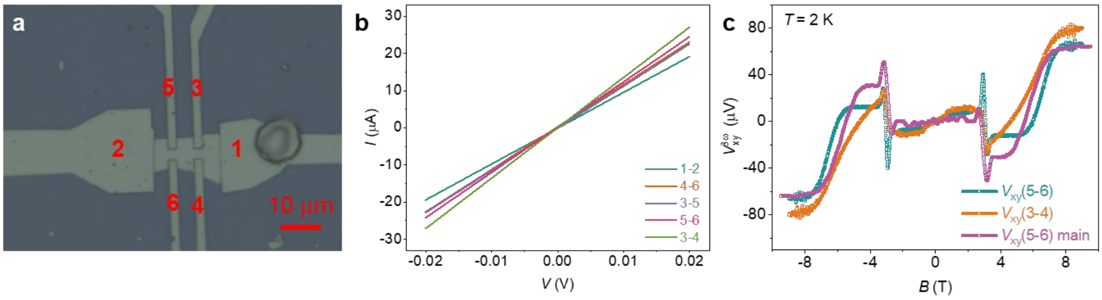

Fig. R4. (a) Optical image of the bulk $MnBi_2Te_4$ devices. Six electrodes are patterned on the bulk $MnBi_2Te_4$ flakes with the number of electrodes being indicated. (b) Two-terminal *I-V* curves of the devices measured between different probes indicated. (c) Third-harmonic nonlinear Hall voltage as a function of the out-of-plane magnetic fields. The cyan and orange curves are measured from the different Hall bar indicated. The purple curve is adopted from the main text and was measured between the same Hall bar probes as that of cyan curve.

[Remark 6]: "Could the authors show the data measured under different frequencies of alternating current? Is the measured nonlinear response independent of the frequency of driving current."

[Reply]: We have measured the frequency dependent third-harmonic nonlinear *I-V* characteristic of bulk $MnBi_2Te_4$ flakes ranging from 73 Hz to 733 Hz for both longitudinal (Fig. R5a) and transverse (Fig. R5b) directions at 2 K and 9 T. As can be seen, all the curves collected at different frequencies are well overlapped, suggesting the nonlinear response of the $MnBi_2Te_4$ flakes is independent of the frequency of driving current. We have added the related measurements as Fig. S5 in the revised Supplementary Information and cited in the revised manuscript on page 6, which reads

"*In addition, the third-harmonic longitudinal and transverse response is independent of the frequency of the driving current, as detailed in Fig. S5 in the Supplementary Note 4.*"

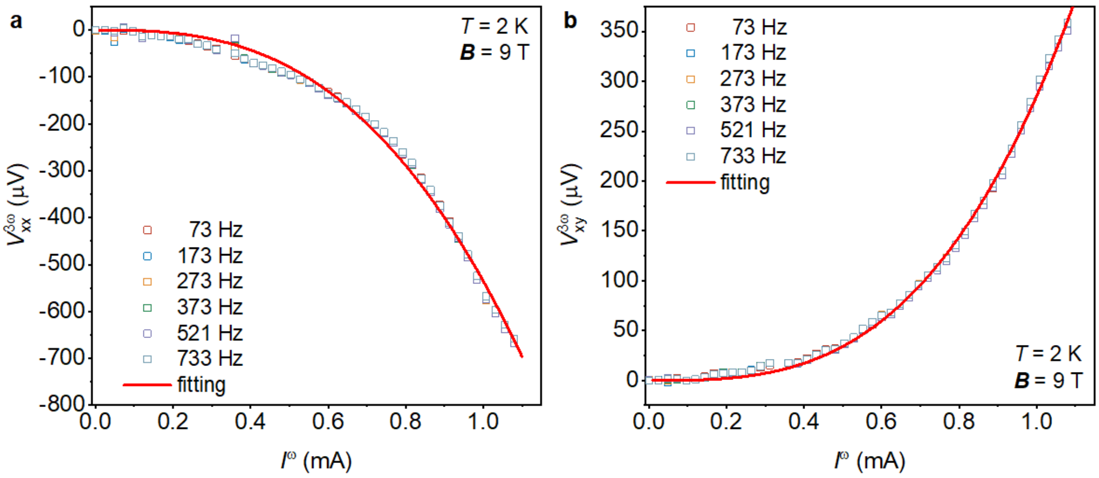

Fig. R5. Third-harmonic nonlinear *I*-*V* characteristic curves of $MnBi_2Te_4$ flakes along longitudinal (a) and transverse (b) directions measured at different frequencies indicated. The red lines are cubic fittings for the data.

[Remark 7]: "As shown in Figure 3b, the calculated σ_{xxxx} contributed by quantum metric does not exhibit a distinct peak when the magnetic state transitions from antiferromagnetic to ferromagnetic. Why there are so sharp peaks observed in $V_{xx}^{3\omega}$ around ± 2.5 T at T = 2 K and 10 K curves, as shown in Figure 3a?"

[Reply]: We thank the reviewer for the constructive comment. As shown in our collected data, such peaks are most prominent at magnetic phase transition from AFM state to canted-AFM state and at low temperatures below 10 K, but get smoothed out for temperatures above 15 K. It hints to us that such a sharp peak feature could be attributed to the phase separation near the magnetic phase transition at low temperatures, such as the formation of multiple small magnetic domains.

When small magnetic domains are formed, electrons can become trapped, leading to the formation of insulating islands. This, in turn, reduces the effective width of the sample for current conduction, while the length remains unchanged. In our experiment, we have fixed the applied current to measure the nonlinear voltage. An investigation into the sample size effect yields

$$\frac{V_{xxxx}^{3\omega}}{(I_x^{\omega})^3} = \frac{L}{(Wt)^3}\frac{\sigma_{xxxx}}{\sigma^4} \quad \text{(Eq. R10)}$$

$$\frac{V_{yxxx}^{3\omega}}{(I_x^{\omega})^3} = \frac{1}{W^2t^3}\frac{\sigma_{yxxx}}{\sigma^4} \quad \text{(Eq. R11)}$$

These equations not only explain the occurrence of sharp peaks in the nonlinear longitudinal and Hall voltages, but also agree with the fact that the peak in the longitudinal voltage, which is proportional to $\frac{1}{W^3}$, is much sharper than the Hall voltage which is proportional to $\frac{1}{W^2}$.

This explanation can be further verified by examining the linear response. A similar analysis yields

$$R_{xx} = \frac{L}{Wt}\rho_{xx} \quad \text{(Eq. R12)}$$

$$R_{xy} = \frac{1}{t}\rho_{xy} \quad \text{(Eq. R13)}$$

This also agrees with our experimental observations that R_{xx} exhibits a small peak near the magnetic phase transition (near 4 Tesla), while R_{xy} does not exhibit any obvious peak structures, as evidenced from measured magnetotransport properties of $MnBi_2Te_4$ in Fig. R6 below.

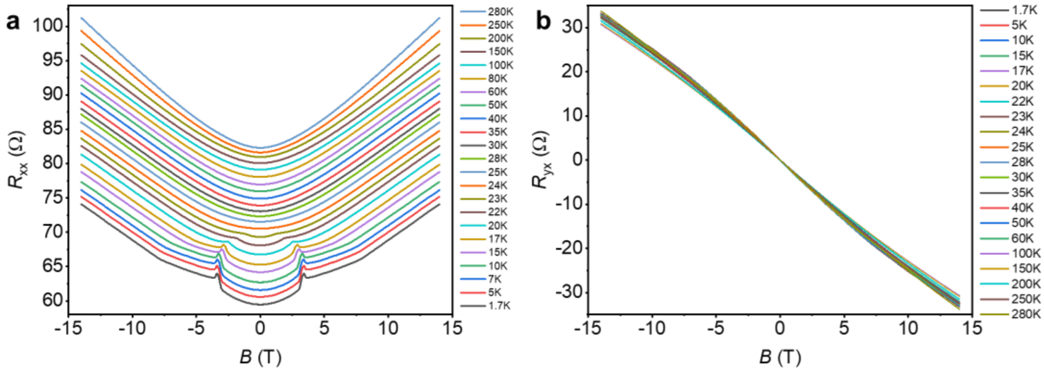

Fig. R6 Magnetotransport properties of bulk $MnBi_2Te_4$. The B-field dependence of (a) longitudinal resistance (R_{xx}) and (b) transverse resistance (R_{yx}) of bulk $MnBi_2Te_4$ measured at different temperatures.

[Remark 8]: "It seems that there are some periodic oscillations in the $V_{xy}^{3\omega}$ curves measured at $T \geq 15$ K in Figure 4a, but no oscillation in the calculated Q_{xxz} at Figure 4b. Can the authors explain where are these oscillations come from?"

[Reply]: We thank the reviewer for pointing out this. After excluding the possible origin from the Shubnikov–de Haas oscillations, which are observed at even higher magnetic field ranges. We believe the occurrence of these oscillations is most likely related to the accuracy of the instrumental measurements. At high temperatures approaching and above the antiferromagnetic transition temperature of bulk $MnBi_2Te_4$, the nonlinear signal becomes relatively weak and much noisier. This introduces some unexpected oscillations in the data anti-symmetrized processes.

[Remark 9]: "Given the authors have theoretically calculated magnetic order parameter Δ dependence nonlinear conductivity originating from quantum metric and Berry curvature quadrupole, the authors should compare the experimental nonlinear conductivity with the theoretically calculated results to see if the experimental data are consistent with the theoretical results."

[Reply]: We thank the reviewer for this important question. We agree with the reviewer that it is important to compare our experimental data and theoretical results. Using a standard four-band Hamiltonian given below, we calculated the nonlinear longitudinal and Hall conductivities. The results are given below. It is important to note that the symmetry and magnitude of the nonlinear conductivities, as a function of (out-of-plane) magnetization order parameter Δ, match the experimental results reasonably well. Importantly, the quantum metric quadrupole contribution and the Berry curvature quadrupole contribution are calculated using exactly the same parameters in the Hamiltonian. The details of the Hamiltonian [given by D. Zhang *et al.*, *Phys. Rev. Lett.* **122,** 206401 (2019)], is given in Table R1 below. The only difference between our Hamiltonian and the one given by D. Zhang *et al.*, is that we used a 1 meV Dirac mass gap M_0^γ instead of a 30 meV mass gap. It is clear that a 30 meV Dirac gap is not possible to be realized experimentally as this will result in a room temperature quantum anomalous Hall state which is not realized experimentally. A 1 meV Dirac mass gap was also assumed in the work of N. Wang *et al.* [This assumption was explained in the Reply to reviewers, in the work of *Nature* **621,** 487–492 (2023)].

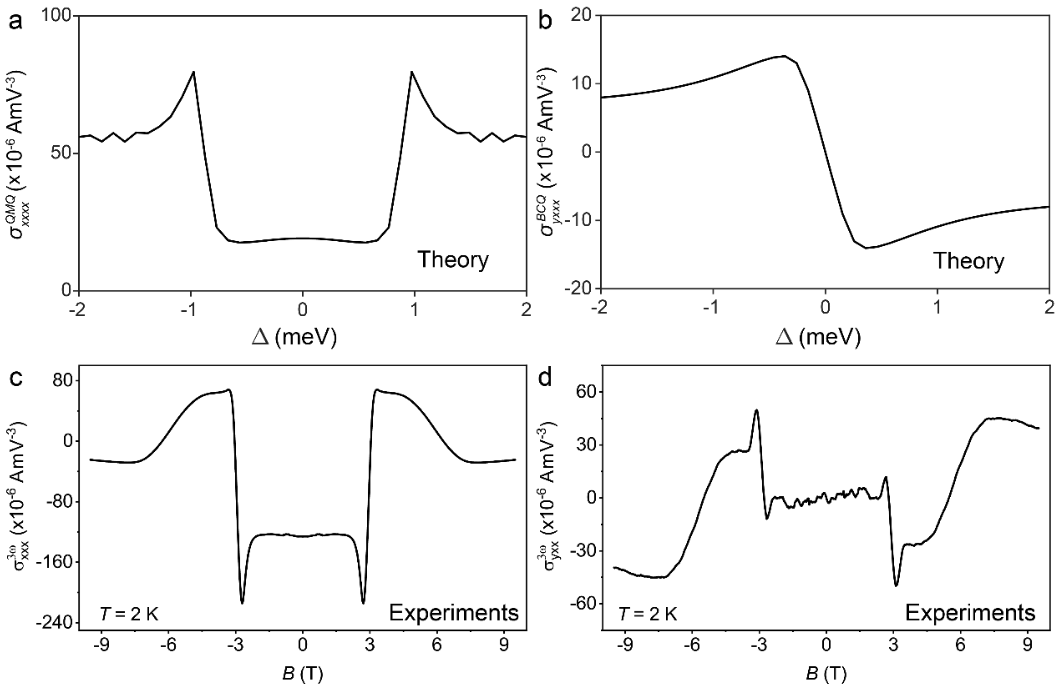

Fig. R7 Quantum metric quadrupole (a), and Berry curvature quadrupole (b) contributions to the third-order nonlinear conductivity from theoretical calculation.

Experimental measured third-harmonic nonlinear longitudinal (c) and transverse (d) conductivity as a function of $\boldsymbol{B}$-fields at 2 K.

It is important to note that at small field, the behavior of the nonlinear Hall conductivity in Fig.R7b and Fig.R7d do not seem to match each other well. This is possibly because, in the presence of the anti-ferromagnetic order, the net magnetization of the spins does not scale linearly with the applied out-of-plane magnetic field at small fields.

Overall, the experimental results match the theoretical calculations reasonably well.

Below are the details of the model used for the nonlinear conductivity calculations.

The effective Hamiltonian of $MnBi_2Te_4$ thin film in our theoretical calculations with a magnetic order Δ induced by the external magnetic field. The effective Hamiltonian is

$$\mathcal{H}(\boldsymbol{k}) = \mathcal{H}_0(\boldsymbol{k}) + \Delta\, \mathcal{H}_{\mathrm{M}}(\boldsymbol{k}) \qquad \text{(Eq. R14)}$$

where

$$\mathcal{H}_0(\boldsymbol{k}) = \epsilon_0(k) + \begin{pmatrix} M_\gamma(k) & A_1 k_z & 0 & A_2 k_- \\ A_1 k_z & -M_\gamma(k) & A_2 k_- & 0 \\ 0 & A_2 k_+ & M_\gamma(k) & -A_1 k_z \\ A_2 k_+ & 0 & -A_1 k_z & -M_\gamma(k) \end{pmatrix} \qquad \text{(Eq. R15)}$$

is the term which preserves the $\mathcal{PT}$ symmetry, and

$$\mathcal{H}_M(\boldsymbol{k}) = \begin{pmatrix} M_1(k) & A_3 k_z & 0 & A_4 k_- \\ A_3 k_z & M_2(k) & -A_4 k_- & 0 \\ 0 & -A_4 k_+ & -M_1(k) & A_3 k_z \\ A_4 k_+ & 0 & A_3 k_z & -M_2(k) \end{pmatrix} \qquad \text{(Eq. R16)}$$

is the part which breaks the time-reversal symmetry.

The basis of the Hamiltonian is $\{|P1_z^+,\uparrow\rangle,\ \ |P2_z^-,\uparrow\rangle,\ \ |P1_z^+,\downarrow\rangle,\ \ |P2_z^-,\downarrow\rangle,\}$. Here, $k_\pm = k_x \pm i k_y$, $\epsilon_0(k) = C + D_1 k_z^2 + D_2(k_x^2 + k_y^2)$, $M_\gamma(k) = M_0^\gamma + B_1^\gamma k_z^2 + B_2^\gamma(k_x^2 + k_y^2)$, $M_{1,2}(k) = M_\alpha(k) \pm M_\beta(k)$, and $M_j(k) = M_0^j + B_1^j k_z^2 + B_2^j(k_x^2 + k_y^2)$ with $j =$

α, β. The parameters for $\mathcal{H}(\boldsymbol{k})$ are listed in Table.R1. Here, we have used a smaller gap M_0^γ to characterize the realistic gap size in our sample. The scattering time we use in the calculation is $\tau = 0.5$ ps.

TABLE R1. Parameters for the effective Hamiltonian $\mathcal{H}(\boldsymbol{k})$ of the $MnBi_2Te_4$ thin film.

C(eV)	D_1(eVÅ^2)	D_2(eVÅ^2)	M_0^γ(meV)	B_1^γ(eVÅ^2)	B_2^γ(eVÅ^2)	A_1(eVÅ)	A_2(eVÅ)
0.0539	-4.0339	4.4250	1	4.2857	8.3750	1.3658	1.9985
M_0^α(eV)	B_1^α(eVÅ^2)	B_2^α(eVÅ^2)	M_0^β(eV)	B_1^β(eVÅ^2)	B_2^β(eVÅ^2)	A_3(eVÅ)	A_4(eVÅ)
-0.1078	0.6232	0.6964	-0.0880	2.7678	1.9650	-0.5450	1.1384

Reply to Reviewer #2 (Remarks to the Author):

[General Remark]: "The manuscript by Li *et al* presents third-harmonic longitudinal and transverse transport measurements of bulk $MnBi_2Te_4$ as a function of magnetic field and temperature, which suggest transitions between antiferromagnetic (AFM), canted antiferromagnetic (CAF) and ferromagnetic (FM) states. Theoretical calculations suggest that these third order signals arise from quantum geometric quadrupoles. The observation of third harmonic signals are quite interesting, and the data presented are nice. The quantum geometric quadrupole effect is novel and exciting. Overall I recommend publication by Nature Communications, if the authors address the following."

[Reply]: We thank the reviewer for recommending publication in *Nature Communications*. As shown in the point-to-point responses below, we have addressed all the comments and suggestions raised by the reviewer, and have revised the manuscript accordingly.

[Remark 1]: "The data presented are very symmetric with respect to ***B***. Are they symmetrized or antisymmetrized? If so, such procedures should be clearly stated in Methods, and raw data shown in Supplement."

[Reply]: The data are symmetrized for longitudinal direction and anti-symmetrized for transverse direction, as indicated below

$$V_{xx}^{3\omega}(B) = \frac{V_{xx}^{3\omega}(B)+V_{xx}^{3\omega}(-B)}{2} \quad \text{(Eq. R17)}$$

$$V_{xy}^{3\omega}(B) = \frac{V_{xy}^{3\omega}(B)-V_{xy}^{3\omega}(-B)}{2} \quad \text{(Eq. R18)}$$

We have added the related descriptions in the Method in the revised manuscript. The raw data are shown in the Supplementary Note 7 in the Supporting Information.

[Remark 2]: "The color scales in Fig. 1a and 1b should be labelled."

[Reply]: Since Fig. 1a and 1b are the schematic demonstration of the Berry curvature of a generic magnetic material with non-zero Berry curvature quadrupoles, the exact value does not have significant physical meanings, but the sign does. Thanks for the reviewer's suggestion, we have added the + and – labels to the color scales in the revised Figs. 1a and 1b to enhance the clarity of the illustrations.

[Remark 3]: "The current applied (0.6 mA) is very large, which may be problematic.
a. For typical R_{xx} ~70 ohms, this translates to 40 mV, which is much larger than thermal energy. Thus the electrons may not be in the ground state.
b. How is heating effect excluded? The authors cite ref. 41, which is a PhD thesis. I suggest the authors include in the Supplement a summary of the relevant sections of the thesis and any representative figures.
c. The Supplement shows that the third harmonic signals are non-linear in current. If a smaller current (e.g. 0.1 mA) is used, does T_N or "switching" field change?"

[Reply]: We thank the reviewer's important comments, we would like to respond these comments from the following aspects:

a. As pointed out by the reviewer, there is a 40 mV voltage difference between the two electrodes, however, it doesn't necessarily mean that the electrons will gain 40 meV kinetic energy under the acceleration, as their momentum will be relaxed by the impurities.

With a scattering time $\tau \sim 0.5$ ps, the estimated kinetic energy gained from the electric field is calculated to be $\varepsilon \sim \frac{(eE_x\tau)^2}{2m_e} = 1$ μeV. Such kinetic energy cannot excite the electrons. In addition, the voltage adopted in our work is consistent with the majority of the community in the nonlinear Hall studies, around 10 ~ 100 mV [*Nature* 565, 337–342 (2019), *Nat. Mater.* **18**, 324–328 (2019), *Nat. Nanotechnol.* 16, 869–873 (2021), *Science* **381**, 181–186 (2023), *Nature* **621,** 487–492 (2023)].

b. We thank the reviewer for pointing out the importance of excluding the heating effect. Generally, the heating effect could amplify the magnitude of the high-order nonlinear signal. We have conducted the first- and third-order magnetotransport measurements with different driving currents of 0.3 mA and 0.6 mA, respectively, as shown in Fig. R8 below. When the applied current in the measurements is reduced from 0.6 mA to 0.3 mA, the heating effect is supposed to be reduced. In this case, the smaller $\frac{V_{xx}^{3\omega}}{(V_{xx}^{\omega})^3}$ and $\frac{V_{xy}^{3\omega}}{(V_{xx}^{\omega})^3}$ ratio is expected to be obtained at lower driving current. However, as shown in Fig. R8b, 8d and 8f, we observed a higher $\frac{V_{xx}^{3\omega}}{(V_{xx}^{\omega})^3}$ and $\frac{V_{xy}^{3\omega}}{(V_{xx}^{\omega})^3}$ ratio for the smaller driving current of 0.3 mA (black curve). This discrepancy implies that the heating effect does not play a prominent role in our experiments.

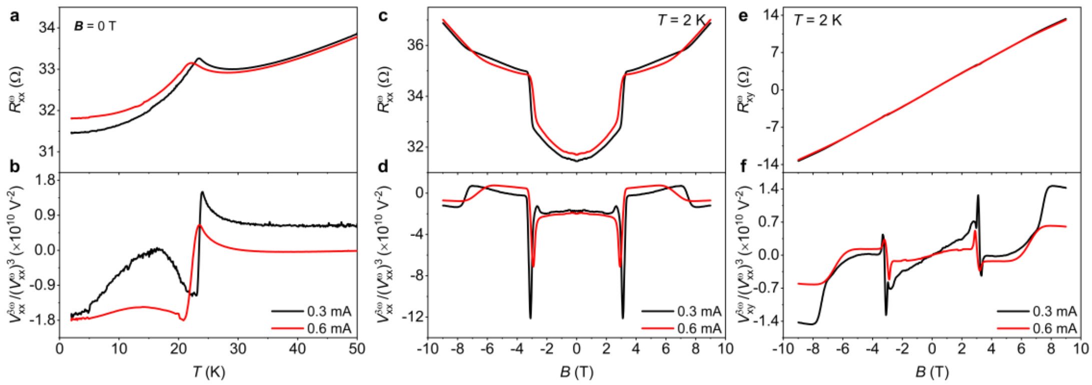

Fig. R8 Transport properties of bulk $MnBi_2Te_4$ under different driving current. First-harmonic longitudinal resistance (a) and third-harmonic longitudinal scaling factor $\frac{V_{xx}^{3\omega}}{(V_{xx}^{\omega})^3}$ (b) of bulk $MnBi_2Te_4$ as a function of temperature measured under 0.3 mA (black curve) and 0.6 mA (red curve), respectively. Magnetic field dependences of first-harmonic longitudinal resistance (c), third-harmonic longitudinal scaling factor $\frac{V_{xx}^{3\omega}}{(V_{xx}^{\omega})^3}$ (d), first-harmonic Hall resistance (e) and third-harmonic transverse scaling factor $\frac{V_{xy}^{3\omega}}{(V_{xx}^{\omega})^3}$

(f) collected under 0.3 mA (black curve) and 0.6 mA (red curve), respectively.

As suggested by the reviewer, we added a section in the Supplementary Note 5 in the revised Supplementary Information to discuss the exclusion of the heating effect.

Concerning Ref. 41, the heating effect was characterized in $MnBi_4Te_7$, which shows similar transport behavior as $MnBi_2Te_4$. It was shown in Ref.41 that, the change in the longitudinal and Hall resistance are insignificant when currents with different magnitudes ranging from 0.2 to 0.6 mA are used to measure the longitudinal resistance and Hall resistance in the presence of different magnetic fields. However, as the measurements performed were for $MnBi_4Te_7$, we decided to remove Ref. 41 from the main text.

c. Since the third-harmonic signal becomes very noisy with smaller driving current of 0.1 mA, we have measured the temperature and magnetic field dependence of the first-harmonic and third-harmonic longitudinal and transverse resistance/voltage under different driving currents of 0.3 mA (black curve) and 0.6 mA (red curve), respectively.

As shown in Fig. R8a and Fig. R8b above, the T_N of bulk $MnBi_2Te_4$ changed very little with increasing driving current from 0.3 mA to 0.6 mA. The switching field of the magnetization transitions of bulk $MnBi_2Te_4$ is almost the same with increasing driving current, as evidenced by the magnetic field dependences of the first-harmonic longitudinal resistance (Fig. R8c) and Hall resistance (Fig. R8e) and the third-harmonic longitudinal scaling factor $\frac{V_{xx}^{3\omega}}{(V_{xx}^{\omega})^3}$ (Fig. R8d) and transverse scaling factor $\frac{V_{xy}^{3\omega}}{(V_{xx}^{\omega})^3}$ (Fig. R8f). Specifically, the overall features of third-harmonic voltages along both longitudinal and transverse directions are well reproducible under external ***B***-fields for different driving currents, which further validate the experimental observations are related to the quantum geometry effect of bulk $MnBi_2Te_4$ rather than stemming from the heating effect. We have added Fig. R8 and relevant discussions in the

Supplementary Note 5 in the revised Supplementary Information.

Reviewers' Comments:

Reviewer #1:
Remarks to the Author:
Authors have answered the previous questions well. I will recommend its publication in NC now.

Reply to Reviewer #1 (Remarks to the Author):

[Remark]: "Authors have answered the previous questions well. I will recommend its publication in NC now."

[Reply]: We thank the reviewer for the positive evaluation of our work.